# *A mineralisation-based method for estimating soil microbial carbon use efficiency*

Soil Biology and Biochemistry 217 (2026) 110143

Contents lists available at ScienceDirect

Soil Biology and Biochemistry

journal homepage: www.elsevier.com/locate/soilbio

# A mineralisation-based method for estimating soil microbial carbon use efficiency

Hanqing Lin, Tom Sizmur, Liz J. Shaw *

*Soil Research Centre, Department of Geography and Environmental Science, University of Reading, Reading, RG6 6UD, UK*

ARTICLE INFO

Dataset link: Data for "A respiration-based method for estimating soil microbial carbon use efficiency" (Original data)

*Keywords:*
Carbon use efficiency
Biosynthesis
Mineralisation
Soil organic carbon
Respiration
Substrate-specific carbon use efficiency

ABSTRACT

Microbial carbon use efficiency (CUE) reflects how microorganisms allocate carbon between mineralisation and biosynthesis, with consequences for soil carbon storage. We present a mineralisation-based $^{13}$C-glucose method that infers substrate-specific CUE from a time series of $^{13}C–CO_2$ alone using a two-component model, thereby avoiding the extraction of microbial biomass $^{13}$C and a fixed $k_{EC}$ conversion factor that is a requirement of widely-used $^{13}$C-biomass/$CO_2$ partitioning methods. Applied to a temperate sandy loam grassland soil, the approach yielded a CUE of $0.80 \pm 0.005$ compared with $0.70 \pm 0.023$ from the conventional 6h-$^{13}$C-biomass/$CO_2$ partitioning approach. The $^{13}$C-mass balance for the mineralisation-based method revealed a greater $^{13}$C recovery (~87%) than for the biomass/$CO_2$ partitioning method (~54%). Because the mineralisation-based estimate integrates intracellular and extracellular biosynthetic products, it provides a less assumption-sensitive CUE under standardised incubations. Furthermore, our method avoids the requirement for labour-intensive fumigation-extraction protocols which currently present a barrier to high throughput CUE estimation of large numbers of soil samples. The reported mineralisation-based CUE value represents a glucose-specific, incubation-condition CUE and should not be interpreted as *in situ* CUE for native SOC.

## 1. Introduction

Soil microbial carbon use efficiency (CUE) is a critical parameter for understanding the transformation of organic carbon substrates into soil organic carbon (SOC) and has major implications for global carbon cycling (Tao et al., 2023). CUE has been defined in various ways. Conceptually, one foundation for CUE terminology followed the formulation used in aquatic microbial ecology, where Del Giorgio and Cole (1998) defined bacterial growth efficiency as the ratio of biomass production to the sum of biomass production and respiration. Here, we adopt a broader, increasingly used, definition in which CUE represents the fraction of carbon taken up in to the cell that is allocated to biosynthesis — including both new biomass and a wide suite of microbial products such as extracellular metabolites and exudates — relative to the total carbon taken up and partitioned between biosynthesis and mineralisation. This broader definition is equivalent to the biochemical efficiency (BE) of Dijkstra et al. (2022), the CUE formulation of Manzoni et al. (2018), and the carbon stabilization efficiency (CSE) of Geyer et al. (2020). Accurately measuring CUE is essential for understanding carbon partitioning in soils, specifically how much carbon is retained in the soil as microbial biomass and microbial products, versus carbon lost to the atmosphere as $CO_2$. This distinction is environmentally relevant given that much of the stable carbon in soils is of microbial origin (Wang et al., 2021).

A widely used method for quantifying microbial CUE in soils is the $^{13}$C-biomass/$CO_2$ partitioning approach. This approach involves tracing the fate of isotopically-labelled C substrates, such as $^{13}$C-glucose, glutamic acid, oxalic acid, or phenol (Frey et al., 2013). In this method, the uptake and mineralisation of $^{13}$C-labelled substrates are monitored, with microbial biosynthesis inferred from the incorporation of $^{13}$C into soil microbial biomass, respiration (mineralisation) measured from $^{13}C-CO_2$ flux, and microbial uptake calculated from the sum of biomass and mineralisation. Microbial biomass carbon (MBC) is typically measured using the fumigation-extraction method (Vance et al., 1987), which quantifies the difference in $K_2SO_4$ extractable organic $^{13}$C between subsamples fumigated with chloroform and unfumigated subsamples (Waldrop and Firestone, 2004; Garcia-Pausas and Paterson, 2011). Respiration is typically measured by analysing the $^{13}C-CO_2$ concentrations in the headspace after incubation in a gas-tight container (Waldrop and Firestone, 2004). In both cases, the measurement is made a few

* Corresponding author.
*E-mail address:* e.j.shaw@reading.ac.uk (L.J. Shaw).

https://doi.org/10.1016/j.soilbio.2026.110143
Received 18 September 2025; Received in revised form 7 March 2026; Accepted 10 March 2026
Available online 11 March 2026

hours after the labelled substrate is added to the soil and is based on the assumption that secondary turnover does not occur (Frey et al., 2013).

A limitation of the $^{13}$C-biomass/$CO_2$ partitioning approach is that, although it in theory produces a CUE estimate consistent with definitions based solely on biomass production (i.e. biomass C/(biomass C + respired C)), it fails to account for extracellular biosynthetic products. MBC reflects biosynthetic products retained within cells — associated with growth, storage, and maintenance — but excludes extracellular products such as extracellular polymeric substances (EPS), which include enzymes, and also low molecular weight compounds. Many of these extracellular products directly or indirectly influence the formation, stabilization and destabilisation of SOC (van Bodegom, 2007; Flemming and Wingender, 2010). Consequently, when CUE is defined to include these extracellular carbon pools (e.g. as in Dijkstra et al. (2022), Manzoni et al. (2018), and Geyer et al. (2020)), relying solely on MBC measurements provides an incomplete picture of microbial carbon allocation and consequently underestimates both CUE and its contribution to long-term SOC sequestration (Craig et al., 2022; Bölscher et al., 2024).

To overcome this conceptual limitation of the current $^{13}$C-based biomass/$CO_2$ partitioning protocols and to obtain an estimate of CUE that captures both intracellular and extracellular biosynthetic products, we devised and tested an alternative $^{13}$C-based approach that estimates biosynthesis indirectly — as the complement of cumulative mineralisation — rather than estimating biosynthesis directly via biomass determination. This approach assumes that all substrate-derived carbon taken up into the microbial cell is ultimately partitioned between mineralisation and biosynthesis. Accordingly, the value we estimate is a substrate-specific CUE, defined as the fraction of added substrate-C retained in microbial biomass and biomass-derived products; for simplicity, we refer to this quantity as CUE throughout.

We incubated soil with $^{13}$C-glucose and measured $^{13}$C-$CO_2$ produced at multiple time points and fitted the resulting data to a two-component kinetic model that represents both the initial phase of direct substrate (glucose) use and the later phase of secondary turnover. From this model, we estimated the proportion of substrate C mineralised during the rapid phase, and defined the complementary fraction as substrate-specific biosynthesis. This operational approach thus provides a CUE estimate compatible with broader definitions that include extracellular carbon pools.

## 2. Materials and methods

### 2.1. Soil samples

Soil samples were collected from a permanent grassland field (5–15 cm) at the University of Reading farm at Sonning, UK (51°28′53.7″N, 0°53′48.8″W). The soil was classified as a sandy loam (64.3 % sand, 34.3 % silt, 1.1 % clay) with pH 6.09 ± 0.03 and organic matter content of 2.81 ± 0.08 %. Samples were sieved while field moist to 4 mm and homogenized before randomly allocating to replicates. The soil characteristics are listed in Table S1.

### 2.2. Experimental design

The experimental design included 6 experimental units (3 with glucose and 3 without glucose) for each of 16 incubation time points (1, 4, 6, 8, 10, 12, 14, 16, 18, 20, 22, 24, 48, 72, 96, and 168 h), resulting in 96 experimental units. Soil (16.29 g fresh weight, equivalent to 15 g dry weight) sub-samples were weighed into 50 mL centrifuge tubes and were amended with 2.28 mL of a solution of glucose (0.82 mg mL$^{-1}$ glucose, 10.9 atom % $^{13}$C) or the equivalent volume of ultra-pure water in order to bring the soil to 80 % of its water-holding capacity. The final soil glucose concentration was 0.12 mg g$^{-1}$ dry soil (equivalent to 50 μg C g$^{-1}$ dry soil) in the 'with glucose' replicates. We conducted a preliminary experiment across a range of glucose additions (0–100 μg C g$^{-1}$ dry soil) to examine how short-term $^{13}$C mineralisation responded to dose and to identify a concentration that would cleanly express the two-component mineralisation signal — an initial exponential phase followed by a near-linear secondary phase — within the experimental duration. Glucose additions that are too high would delay the emergence of the secondary phase beyond our sampling window, whereas additions that are too low would fail to capture a clear exponential phase, reducing model identifiability (Fig. S1). On this basis, we selected 50 μg C g$^{-1}$ dry soil, the same concentration used by Frey et al. (2013), to also ensure comparability with previous studies. This concentration (approximately 10 % of microbial biomass C) has been shown to have no significant effect on microbial biomass C or microbial community composition (PLFA profiles) (Brant et al., 2006), consistent with the interpretation of Geyer et al. (2019) that any new growth stimulated by glucose addition is counterbalanced by concurrent losses of C from the biomass pool.

Following the addition of glucose or water, the tubes were sealed with Suba-Seal® septum stoppers. All samples were incubated at 20 °C in darkness. A headspace gas sample for determination of respired $CO_2$ (Section 2.3) was collected at the start and end of the incubation time allocated to that sample. After the headspace gas sampling at the end of the incubation period, each soil sample was divided into two representative sub-samples. One sub-sample was used to determine microbial biomass carbon (Section 2.4), and the remaining sub-sample was frozen at −20 °C to measure the total carbon in the soil (Section 2.5). Subsequently, all respired $CO_2$, microbial biomass carbon, and total carbon samples were analysed for $\delta^{13}$C.

### 2.3. Soil $CO_2$ production measurements

Immediately after placing the septa over the tube at the start of the incubation, 15 mL of $N_2$ was injected, and the syringe plunger was moved up and down several times to mix the gasses before sampling 15 mL of headspace gas ($T_0$ sample) and injecting it into a vacuumed 12 mL Exetainer® vial (Labco Ltd, High Wycombe, UK) to create overpressure.

At the end of the incubation period (after 1, 4, 6, 8, 10, 12, 14, 16, 18, 20, 22, 24, 48, 72, 96, or 168 h), the injection of 15 mL of $N_2$, mixing of headspace gas, and sampling was repeated to collect a $T_1$ sample. Headspace gas samples were stored at 20 °C before analysis using an Agilent 7890B Gas Chromatograph (GC) system. Sample aliquots (1 mL) were injected into the GC system by an autosampler under the following conditions: front SS inlet $N_2$, mode split, heater at 100 °C, pressure of 33.2 psi, total flow of 40 mL min$^{-1}$, and septum purge flow of 2 mL min$^{-1}$. The samples were then separated using a J&W GC packed column with UltiMetal tubing (12 ft length, 1/8 in. OD, 2 mm ID) packed with Hayesep Q (mesh size 80/100). $CO_2$ was analysed by a Flame Ionization Detector (FID) set to 250 °C, with $H_2$ flow at 50 mL min$^{-1}$, air flow at 450 mL min$^{-1}$, and makeup flow at 2 mL min$^{-1}$, following its catalytic conversion to $CH_4$ using a methanizer to enable detection and quantification. The system was calibrated with 506 ppm, 2539 ppm, and 5066 ppm $CO_2$ gas standards.

After GC-FID analysis, headspace gas samples were then stored again at 20 °C before analysis using a ThermoFisher Scientific Delta V IRMS, with sample introduction using a Gas Bench II setup. Calibration was performed using IAEA 603 (calcium carbonate, $\delta^{13}C = +2.46$ on the VPDB scale), IAEA 610 (calcium carbonate, $\delta^{13}C = -9.109$) and IAEA 612 (calcium carbonate, $\delta^{13}C = -36.722$) standards. Standards were prepared by adding 0.1 mg of calcium carbonate ($CaCO_3$) powder to a 12 mL Exetainer® vial. The vial was then sealed with a cap and placed into the autosampler of the gas bench. Vials were then flushed with helium for 5 min to remove air and, following this, six drops of phosphoric acid ($H_3PO_4$) were added to liberate the $CaCO_3$ as $CO_2$, ensuring even distribution of the acid around the bottom of the vial. Calibration standards were introduced into the source 10 times at both the beginning and the end of each run. Data were processed using Isodat Gas Isotope Ratio Mass Spectrometry software (ThermoFisher Scientific) to generate $\delta^{13}$C values.

### 2.4. Microbial biomass carbon

Soil samples for microbial biomass carbon measurements were divided into unfumigated and fumigated subsamples. For each unfumigated subsample, 6.19 g (equivalent to 5 g dry weight) of incubated soil was weighed into a 50 mL centrifuge tube. After shaking the soil with 20 mL of 0.5 M $K_2SO_4$ for 30 min, the mixture was filtered, and an aliquot was analysed for dissolved organic carbon (DOC) using a Shimadzu TOC-L analyser. For the fumigated subsamples, the same mass of soil was weighed into 25 mL glass crystallizing dishes (Firmasil) then fumigated with chloroform in a vacuum desiccator under dark conditions for 24 h, before running the same $K_2SO_4$ extraction and analysis process (Vance et al., 1987). The microbial carbon flush (difference in extractable carbon between fumigated and unfumigated samples) was converted to microbial biomass carbon using a $k_{EC}$ factor of 0.45 (Joergensen, 1996).

To determine the $\delta^{13}C$ of each microbial biomass carbon extraction sample, the method of Garcia-Pausas and Paterson (2011) was followed with slight modification. A 1 mL aliquot of the extract solution was dispensed into a 15 mL glass vial. Dissolved inorganic carbon was removed by adding 0.5 mL of 1.3 M phosphoric acid, followed by a 10-min reaction at room temperature. The vial was then capped, vacuumed, and injected with 15 mL $N_2$. To evolve organic carbon as $CO_2$, 1 mL of 1.05 M sodium persulfate ($Na_2S_2O_8$) was injected into the solution through the rubber septum of the vial cap. The sample was then heated in a dry block at 90 °C for 30 min. The vial was flushed with 15 mL of $N_2$ using a syringe, with the syringe plunger moved up and down several times before sampling 15 mL of headspace gas released from the extract. This 15 ml headspace gas sample containing $CO_2$ was then injected into a vacuumed 12 mL Exetainer® vial (Labco Ltd, High Wycombe, UK) to create overpressure. The $\delta^{13}C$ of the $CO_2$ sample was determined using GC-IRMS, as described in Section 2.3.

### 2.5. Soil organic carbon

Soil samples were stored at −20 °C and subsequently freeze-dried at −50 °C for 48 h using a Heot Powerdry PL3000 freeze dryer. Freeze-dried soils were ground with a Fritsch P-5 planetary mill at 300 rpm for 3 min, passed through a 0.5 mm sieve, homogenized, and stored in a desiccator at 20 °C prior to analysis.

For $\delta^{13}C$ and soil organic carbon (SOC) analysis, 10 mg of freeze-dried soil powder was weighed into a tin capsule and introduced into a ThermoFisher Scientific Delta V IRMS coupled to a Flash EA 1112 HT elemental analyser via a Conflo IV interface. Samples were combusted to $CO_2$ in the EA and the $CO_2$ was admitted to the IRMS for isotope-ratio determination; automatic dilution (Smart EA) was used when necessary to keep peak amplitudes within the linear range. A TC/EA module is available on the system but was not used for $\delta^{13}C$ measurements in this study. $\delta^{13}C$ values are reported relative to VPDB using Isodat.

SOC content was quantified using the Flash EA 1112 HT based on thermal conductivity detection. The $\delta^{13}C$ values were derived from IRMS outputs and processed using Isodat software (ThermoFisher Scientific) and are reported relative to the VPDB standard. Calibration was performed using three carbonate standards (IAEA 603, IAEA 610, and IAEA 612), each prepared by encapsulating 0.4 mg of $CaCO_3$ in a tin capsule.

### 2.6. Calculation of $^{13}C$-labelled carbon isotope composition and model fitting

By modifying the Waldrop and Firestone (2004) method, the percentage of C derived from the added glucose was calculated using the following formula:

$$\%C_{glucose} = \left[\frac{\left({}^{13}C\%_G - {}^{13}C\%_C\right)}{\left({}^{13}C\%_{glucose} - {}^{13}C\%_C\right)}\right] \times 100\% \quad (1)$$

where ${}^{13}C\%_C$ is the atom % $^{13}C$ value of the C produced by the control (no-glucose) soils (1.08 atom % $^{13}C$), ${}^{13}C\%_G$ is the atom % $^{13}C$ value of the C produced by the glucose treatment soils, ${}^{13}C\%_{glucose}$ is the atom % $^{13}C$ value of the labelled glucose (10.9 atom % $^{13}C$), and the atom % $^{13}C$ value was calculated from $\delta^{13}C$ (‰) using standard equations based on the VPDB reference ratio.

The cumulative % of glucose-C mineralised after a given incubation time point is calculated as:

$$\%mineralised = \frac{\%C_{glucose}}{m_{Glucose-C}} \cdot \frac{V \cdot C_{CO_2,T_1} \cdot M_{mol}(C)}{W \cdot M_{mol}(CO_2)} \quad (2)$$

Where $\%C_{glucose_{CO_2}}$ is the percentage of $CO_2$-C derived from the added glucose (Eq. (1)), $m_{Glucose-C}$ is the mass (μg) of added glucose-C in glucose treatment samples, $V$ is the volume of the headspace in the centrifuge tube (L), $C_{CO_2,T_1}$ is the $CO_2$ concentration after incubation in mol $CO_2$ $L^{-1}$, $M_{mol}(C)$ is the molar mass of carbon, $W$ is the dry weight of the soil in kg and $M_{mol}(CO_2)$ is the molar mass of carbon dioxide.

To estimate the proportion of SOC derived from the added $^{13}C$-labelled glucose, the following isotope mixing model was applied (Balesdent and Mariotti, 1996):

$$SOC_{glucose} = \%C_{glucose_{SOC}} \cdot SOC \quad (3)$$

Where $\%C_{glucose_{SOC}}$ is the percentage of SOC derived from the added glucose (Eq. (1)), $SOC$ is the total soil organic carbon content (μg C $g^{-1}$ dry soil).

### 2.7. Calculation of CUE using the two-component kinetic model

Glucose-derived C mineralised at each time point was fitted to a two-component model (Fig. 1) using Origin's Nonlinear Curve Fit functionality.

$$Mineralisation = a \cdot (1 - exp(-b \cdot t)) + (y0 \cdot t) \quad (4)$$

where *Mineralisation* is the proportion of the glucose-C added that has been respired over the incubation time $t$, $a$ is the asymptotic maximum as a proportion of added glucose-C mineralised directly from the

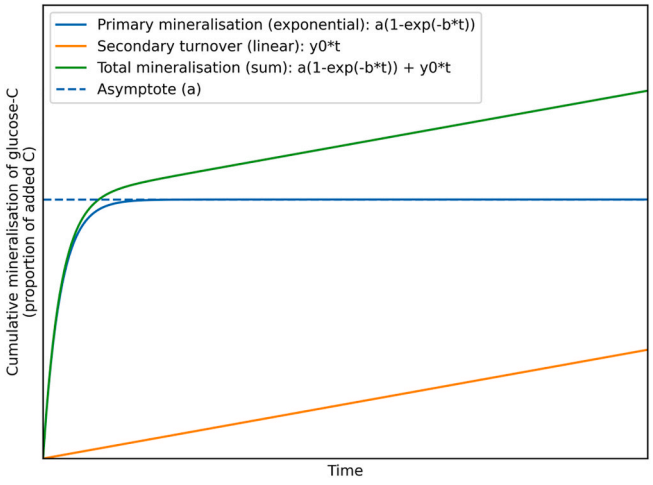


**Fig. 1.** Schematic representation of the two-component kinetic model used to describe cumulative mineralisation of glucose-C. The exponential term represents primary substrate mineralisation approaching asymptote (a), while the linear term represents secondary turnover of substrate-derived biosynthetic products. The total curve equals the sum of both components.

substrate pool (cumulative contribution of first component); $b$ is the rate constant describing this direct mineralisation of the added glucose-C (first component, exponential phase), $y0$ is the constant rate of secondary turnover of glucose-derived-C that has been incorporated in to biosynthetic products and then turned over and mineralised (second component, linear phase), and $t$ is time after substrate addition to soil.

Carbon Use Efficiency (CUE) is then calculated as follows:

$$CUE = 1 - a \quad (5)$$

where CUE is the microbial Carbon Use Efficiency of glucose in soil, defined here as fraction of carbon taken up in to the cell that is allocated to biosynthesis relative to the total carbon taken up and partitioned between biosynthesis and mineralisation.

The crossover time ($t_{crossover}$) was also calculated as described in the Supplementary Materials (Eq. S(5)). This $t_{crossover}$ is mathematically defined as the time at which the instantaneous rates of the two components are equal and can be interpreted as the shift from $CO_2$ production being dominated by direct mineralisation of added substrate (first component) to a slower phase dominated by the mineralisation of substrate-derived carbon that had been incorporated into biosynthetic products (second component).

### 2.8. Calculation of CUE using the partitioning method

CUE was also determined by method of Frey et al. (2013) using $^{13}CO_2$-C and $^{13}$C-microbial biomass carbon values for an incubation time of 6 h. Using $K_2SO_4$ extracts from the glucose-treated and control (no-glucose) samples, the proportional contribution of glucose carbon to the total extracted carbon ($\%C_{glucose}$) was calculated for both unfumigated and fumigated $K_2SO_4$ extracts using Eq. (1). The glucose-derived C of the microbial biomass carbon ($MBC_{glucose}$) was then calculated using a modification of the Waldrop and Firestone (2004) and Garcia-Pausas and Paterson (2011) methods:

$$MBC_{glucose}\left(\mu g\ C\ g^{-1}\ dry\ soil\right) = \frac{\left[\left(\%C_{glucose_F} \cdot DOC_F\right) - \left(\%C_{glucose_{UF}} \cdot DOC_{UF}\right)\right]}{k_{EC}} \quad (6)$$

where $\%C_{glucose_F}$ and $\%C_{glucose_{UF}}$ are the percentage of extractable organic carbon in fumigated (F) and unfumigated (UF) extracts derived from the added glucose (Eq. (1)), $DOC_F$ and $DOC_{UF}$ are the fumigated and unfumigated extracted dissolved organic carbon concentration (μg C $g^{-1}$ dry soil), respectively, measured on a soil dry mass basis. A $k_{EC}$ value of 0.45 was used, following Joergensen (1996).

CUE was then calculated as follows:

$$CUE = \frac{MBC}{MBC + \sum CO_2 - C} \quad (7)$$

where $MBC$ is the amount of glucose-derived C in microbial biomass carbon, $\sum CO_2 - C$ is the amount of glucose-derived C respired during the incubation time.

### 2.9. Statistical analysis

All statistical analyses were performed using Microsoft Excel and OriginPro 2025 (OriginLab Corporation, Northampton, MA, USA). The 95 % confidence interval (CI) for the two-component model was computed using Origin's Delta method to propagate the parameter uncertainties, thereby providing a smooth and continuous measure of the prediction precision across the time span. In addition, a 95 % prediction interval (PI) was calculated to reflect the expected range of future observations by incorporating both parameter uncertainty and residual variance, offering a more comprehensive assessment of model reliability. The adjusted $R^2$ was calculated to quantify the model's fit to the data. All glucose-C mineralisation measurements (n = 48) across all sampling times were used for model parameter estimation ($a$, $b$, and $y0$) and to characterise soil mineralisation dynamics. The two-component model was fitted in OriginPro using nonlinear regression, which produced parameter estimates and their standard error via the Delta method. The mineralisation-based CUE ($CUE_{model}$) was then calculated as $CUE_{model} = 1 - a$ (Eq. (5)). Because this is a linear transformation, the standard error of $CUE_{model}$ is equal to the standard error of parameter $a$.

For comparability with previous glucose-based $^{13}$C-CUE studies – most of which are based on short term incubations, typically around 6 h (e.g. Frey et al. (2013)) – we compared CUE values derived from the two-component model with those obtained using the 6-h $^{13}$C-biomass/$CO_2$ partitioning method. To maintain statistical independence between methods, the 6-h point was excluded when fitting the two-component model. Agreement between the two estimates was then evaluated using a two-tailed $t$-test. The two-component model parameter a was estimated by fitting the model (Equation (4)) to the experimental data (n = 45, all time points except 6-h). In parallel, the partitioning method provided direct measurements, and repeated experiments yielded the corresponding mean values and standard errors (n = 3). The difference between the model-derived parameter ($1 - a$, Eq. (5)) and the experimentally measured value was standardized by combining their respective uncertainties. The test statistic and approximate degrees of freedom were calculated using the Welch-Satterthwaite approach (Satterthwaite, 1946; Welch, 1947) as described in the Supplementary materials. Using the computed t-statistic (4.33) and the approximated degrees of freedom (2.20), the two-tailed p-value was determined from the t-distribution. A p value lower than 0.05 was used as a threshold to consider differences as statistically significant.

Sensitivity analysis was conducted to assess the stability of the two-component model parameters under reduced data availability, using both random and systematic removal of time points (see Supplementary Materials).

## 3. Results

### 3.1. Glucose-derived carbon mineralisation and two-component kinetic model fitting

The mineralisation of $^{13}$C-labelled glucose increased rapidly during the first 10 h and then slowed over time, transitioning to a slower, approximately linear, phase of mineralisation. The two-component

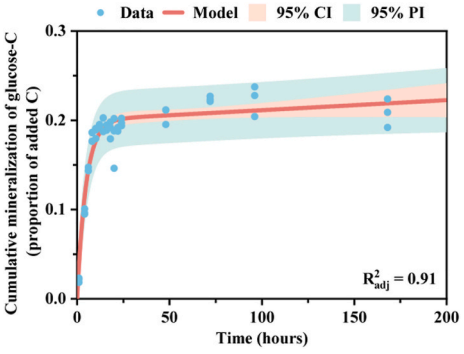


**Fig. 2.** Glucose-derived carbon mineralisation, expressed as a proportion of the initially added glucose-C, and two-component model fitting over time. Blue dots are glucose-derived $CO_2$-C flux as a proportion of added glucose-C. The red line is the fitted model curve through the blue dot data. The pink shaded area indicates the 95 % confidence interval (95 % CI) of the model fit, reflecting the uncertainty in parameter estimation. The aqua shaded area represents the 95 % prediction interval (95 % PI), indicating the expected range for future observations by incorporating both parameter uncertainty and residual variation. n = 3 for each time point, with all points plotted on the figure. (For interpretation of the references to colour in this figure legend, the reader is referred to the Web version of this article.)

model (Eq. (4) in Section 2.7) provided a good fit to the experimental data ($R^2_{adj} = 0.91$, Fig. 2). The estimated model parameters were $a = 0.20$, $b = 0.21$, and $y0 = 0.00011$ (Table 1). The value of parameter a (0.20) allows us to calculate CUE, using the relationship defined in Eq. (5), to be 0.80 or 80 %. The time point $t_{crossover}$ (when the instantaneous rates of primary and secondary mineralisation components are equal) was calculated as 28.3 h after the start of the experiment. $CO_2$-C flux (μg C $kg^{-1}$ dry soil $h^{-1}$) and accumulated $CO_2$-C flux (μg C $kg^{-1}$ dry soil) data for both glucose-amended and non-amended soils are provided in the Supplementary Materials (Fig. S2 and S3).

### 3.2. Comparison between the CUE calculated using the two-component kinetic model and the partitioning method

To evaluate the performance of the two-component kinetic model method relative to the 6-h incubation $^{13}$C-biomass/$CO_2$ partitioning method (see Section 2.8), we compared the CUE values obtained from both approaches using the same soil samples. The two-component model method yielded a mean CUE of 0.80 ± 0.0052 (SE), while the partitioning method resulted in a mean CUE of 0.70 ± 0.023 (SE) (Fig. 3). A two-tailed *t*-test resulted in a p-value of 0.0495, which lies close to the conventional 0.05 threshold and provides modest statistical evidence for a difference between the two methods.

### 3.3. Glucose-derived C mass balance

The mass balance recovery of glucose-derived carbon over the 168-h incubation period was evaluated in two ways. For the $^{13}$C-biomass/$CO_2$ partitioning method, recovery was calculated as the sum of glucose-derived C in non-fumigated $K_2SO_4$-extractable organic carbon ($DOC_{UF}$), microbial biomass carbon (MBC) and the cumulative $CO_2$-C (Fig. 4A). For the two-component kinetic model method, recovery was calculated as the sum of glucose-derived C in $CO_2$-C and the SOC (Fig. 4B). For the $^{13}$C-biomass/$CO_2$ partitioning method, the percentage of added glucose-C recovered as non-fumigated extractable organic carbon declined rapidly from 8 % at 1 h to below 0.5 % after 8 h. Carbon in MBC increased sharply during the first 8 h, peaking at 45 %, and remained above 27 % for the remainder of the incubation. Glucose-derived $CO_2$ accumulated over time, reaching 21 % at 168 h (Fig. 4A). In contrast, the two-component model-based method, which measured (via EA-IRMS) the total C retained in soil organic carbon, regardless of extractability, showed a more stable pattern. Total glucose-derived SOC fluctuated between 75 % and 62 % of the added C over the course of the incubation (Fig. 4B). When the two methods were compared, the partitioning method-based approach (reflecting mass balance of the $^{13}$C-biomass/$CO_2$ partitioning method) consistently resulted in lower total added C recovery (approximately 55%) than the two component model-based method (reflecting mass balance of the two-component kinetic model method; approximately 85 %), with differences between the approaches averaging over 30 % across time points (Fig. 4C).

## 4. Discussion

### 4.1. Interpretation of the two-component model CUE estimation

We applied a two-component kinetic model to glucose-derived $CO_2$ flux data based on the assumption that mineralisation can be represented as two separable metabolic components: (i) an initial exponential phase dominated by direct mineralisation of the substrate carbon and (ii) a second approximately linear phase dominated by the secondary turnover of microbial biomass and biomass-derived products that were biosynthesised from that substrate carbon. The model therefore assumes that these processes contribute additively to total $CO_2$ production and can be distinguished kinetically, such that secondary turnover does not alter the estimated magnitude of the initial substrate mineralisation component. Our approach further assumes that all added substrate-C is consumed and partitioned between mineralisation and biosynthesis, with no free substrate remaining in soil. That the initial component is assumed to follow exponential kinetics is consistent with first-order substrate turnover, where the rate of $CO_2$ production is proportional to the substrate concentration rather than being constrained by microbial growth. As discussed earlier (section 2.2), the concentration of glucose C added (approximately 10 % of microbial biomass C) has previously been shown to have no significant effect on microbial biomass C (Brant et al., 2006). The observed biphasic pattern of mineralisation (Fig. 2) supports the suitability of our two-component model. Similar dynamics, characterized by rapid initial substrate mineralisation superseded by a slower secondary phase, have been reported in earlier studies with substrates such as phenol, aniline, benzylamine, nitrilotriacetic acid, 2,4-Dichlorophenol, *p*-Nitrophenol (Scow et al., 1986), glucose, starch, cinnamic acid, and stearic acid (Jagadamma et al., 2014).

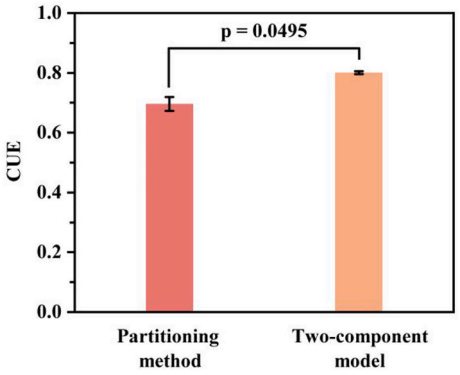


**Fig. 3.** Comparison of CUE values between the mineralisation-based two-component kinetic model method ($CUE_{model} \pm SE_{model}$, from the nonlinear fit) and the 6-h incubation $^{13}$C-biomass/$CO_2$ partitioning method (mean ± SE of three replicates).

To our knowledge, few studies have proposed kinetic modelling of mineralisation data with isotopic tracers to estimate CUE. One exception is Mariano et al. (2016), who fitted a double-exponential decay model $f = (a_1 \cdot e^{-k_1 t}) + (a_2 \cdot e^{-k_2 t})$ to the proportion of glucose-$^{14}$C remaining in soil over time. In their framework, the parameter $a_1$ — consistent with our interpretation — represented the fraction of tracer rapidly mineralised via catabolic processes, while $a_2$ represented the fraction allocated anabolically into microbial biomass and subsequently mineralised more slowly through turnover. CUE was then calculated as $a_2/(a_1 + a_2)$. However, Mariano et al. (2016) did not compare this kinetic approach with the more widely used partitioning method, nor did they assess mass balance.

During the initial phase, the added glucose is rapidly taken up by microorganisms, as evidenced by the proportion of glucose-derived carbon in the non-fumigated extractable pool declining to less than 0.5 % of the initial input within the first 8 h (Fig. 4A). Previous studies have consistently shown that added glucose is rapidly depleted, typically within 0.5 to 12 h (Coody et al., 1986; Nguyen and Guckert, 2001; Hill et al., 2008). Although a minor fraction of glucose may be transiently sorbed to soil particles, primarily via hydrogen bonding on non-charged mineral surfaces (Islam et al., 2023), microbial uptake of glucose generally outcompetes sorption processes in soil (Fischer et al.,

**Table 1**
Estimated parameters of the two-component model. Data are mean ± standard error (n = 48). Parameters *a* and *b* were significantly different from zero ($p < 0.05$), whereas *y*0 was not significantly different from zero (p = 0.083).

| Parameter | *a* | *b* | *y*0 |
|---|---|---|---|
| Value | 0.20 ± 0.0049 | 0.21 ± 0.018 | 0.00011 ± 0.000064 |

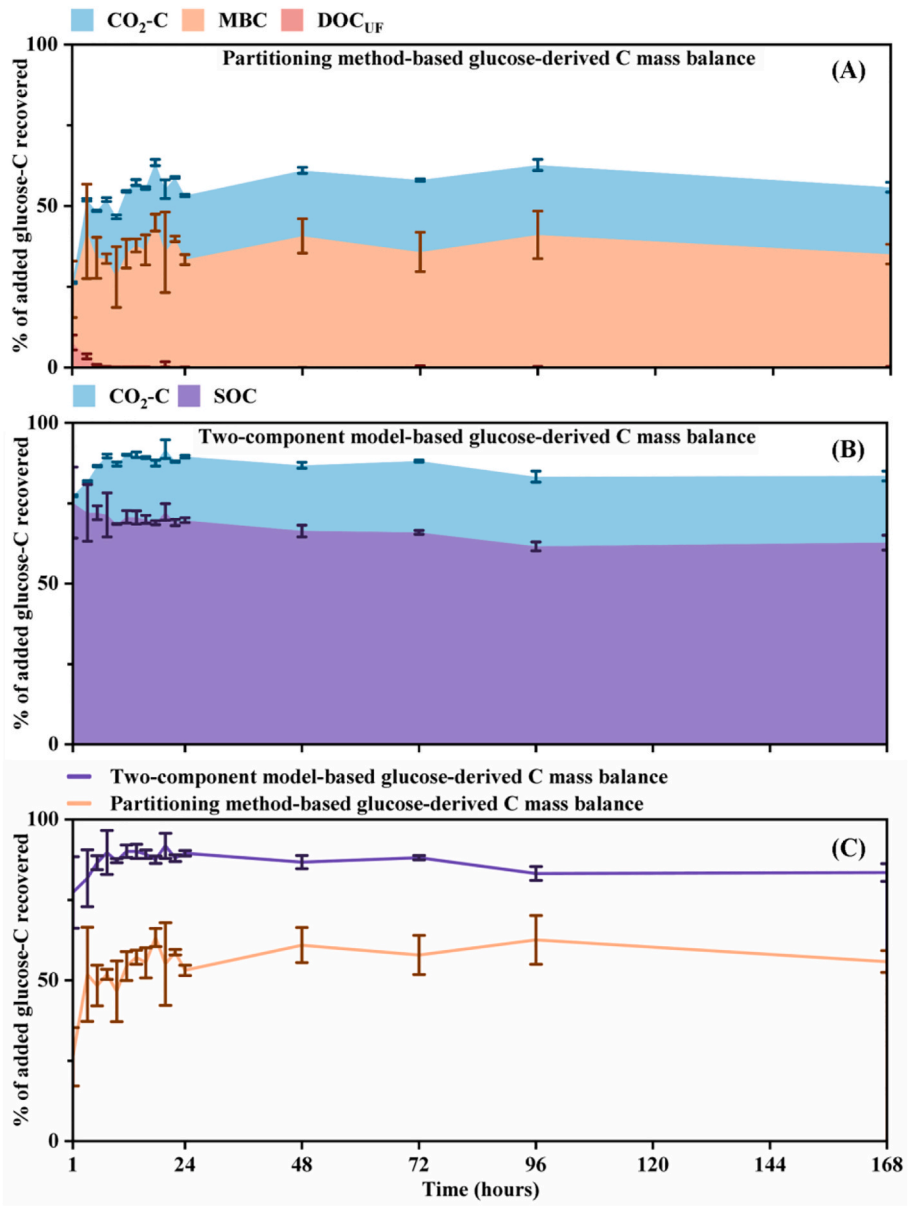


**Fig. 4.** Cumulative recovery of glucose-derived carbon under two carbon accounting frameworks. For the $^{13}$C-biomass/$CO_2$ partitioning method glucose-derived carbon mass balance (A), carbon pools include non-fumigated $K_2SO_4$-extractable organic carbon ($DOC_{UF}$) (red area), microbial biomass carbon (MBC) (orange area), and $CO_2$–C (blue area). For the two-component model-based glucose-derived carbon mass balance (B), carbon pools include soil organic carbon (SOC) (purple area) and $CO_2$–C (blue area). For both (A) and (B), carbon pools are expressed as a proportion of added glucose-C. Shaded areas represent the cumulative contribution of each carbon pool; the total stacked area indicates the total recoverable carbon. Error bars represent the standard deviation of the mean (n = 3 for each time point). Panel (C) represents the comparison of total carbon recovery under the two approaches. Values indicate the mean cumulative recovery (%) of added glucose-C with error bars showing standard deviation. (For interpretation of the references to colour in this figure legend, the reader is referred to the Web version of this article.)

2010). Therefore, any remaining free glucose in the soil that is not taken up by microorganisms is likely to be negligible. While the rapid disappearance of extractable glucose-C indicates efficient microbial uptake, our mineralisation-based approach cannot resolve the intracellular fate of glucose once it has entered the cell. Specifically, it is not possible to distinguish whether assimilated glucose is allocated to growth, temporary intracellular storage, or other biosynthetic products. More mechanistic methods, such as metabolic flux analysis, are required to disentangle these intracellular allocation pathways. For example, Dijkstra et al. (2015) used stable-isotope-enabled flux analysis to show that, under glucose addition, microbial carbon was channelled directly into metabolism with little evidence for the formation of reserve pools. The rapid phosphorylation of glucose upon uptake and its immediate entry into central metabolism are supported by microbial physiology (Deutscher et al., 2006; Lane et al., 2018) and are consistent with the view that intracellular free glucose pools are short-lived. This phosphorylation also initiates catabolite repression, suppressing the uptake of most non-glucose carbon sources and further enhancing glucose uptake efficiency (Deutscher et al., 2006; Lane et al., 2018; Wijnants et al., 2020; Roth et al., 2024).

In our two-component kinetic model, the crossover time ($t_{crossover}$) between the two mineralisation phases occurred at approximately 28 h after glucose addition. This marks the transition from $CO_2$ production dominated by direct mineralisation of the added substrate to $CO_2$ production being dominated by a slower phase dominated by mineralisation of substrate-derived biosynthetic products. Identification of $t_{crossover}$ is therefore important for constraining the relative contributions of the two components for the reliable estimation of parameter *a*, which

represents the size of the first component, that is, the proportion of substrate-C that we infer is mineralised as a result of initial mineralisation. The timing of $t_{crossover}$ is a function of glucose uptake kinetics and subsequent metabolism, influenced by the concentration of glucose added, temperature and factors affecting the bioavailable glucose concentration in soil pore water, such as moisture, clay content, and mineralogy (Coody et al., 1986; Nguyen and Guckert, 2001; Porras et al., 2018). In addition, initial microbial activity and cellular constraints — including toxicity (Bardgett and Saggar, 1994) and other physiological limitations (Deutscher et al., 2006; Lane et al., 2018) — can modulate the timing of this shift (Mariano et al., 2016). When applying the method beyond the conditions tested here, we therefore recommend first conducting a pilot incubation to approximate the timing of the crossover. If $t_{crossover}$ can be reasonably estimated from prior information from similar soils and conditions, sampling can be focused around the expected crossover, potentially reducing the total number of time points (see also discussion in section 4.3 on reduction of sampling times). This preliminary step does not necessarily require $^{13}C$ labelling, as a likely time range in inflection in $CO_2$ production rates can be identified from mineralisation measurements alone (Fig. S4). Subsequent sampling can then be designed to ensure adequate coverage both before and after the estimated crossover period.

The soil microbial CUE estimated from our two-component model should also be interpreted specifically within the defined incubation context (50 μg glucose-C $g^{-1}$ dry soil, 80% WHC, 20 °C, in darkness). Glucose is a highly bioavailable substrate that is energetically favourable and is therefore typically metabolised with a high CUE (Gommers et al., 1988). However, caution should be applied when inferring actual CUE of microbial communities found across various soil types and environmental conditions. Microbial CUE has been shown to vary with substrate quality, community composition, and environmental constraints such as soil texture, pH, moisture, and nutrient status (Manzoni et al., 2012; Sinsabaugh et al., 2013; Islam et al., 2023; Zhang et al., 2024; Liang et al., 2025). In non-amended soils, dissolved organic matter consists of a diverse range of biomolecules. Some of these molecules are more energy-limited and therefore more recalcitrant than glucose, which usually leads to a lower CUE (Gommers et al., 1988; Sinsabaugh et al., 2013). Thus, the CUE measurement derived here should not be viewed as representative of *in situ* soil conditions, but rather as a potential or upper-bound estimate under conditions of high substrate quality. This makes it useful for comparative analyses across soils or treatments under standardized laboratory conditions.

The two-component model approach also provides a parameter $y0$ that is interpreted to represent the rate of secondary turnover — i.e. the gradual mineralisation of microbial products previously synthesized from the added glucose. In our dataset, $y0$ was not statistically significantly different from zero over the 168 h incubation. This suggests that secondary turnover of glucose-derived residues made only a minor contribution to the short-term C balance in our experiment and that longer incubations may be required to resolve y0 statistically.

Temporal patterns in CUE estimated using the $^{13}C$-biomass/$CO_2$ partitioning method provide further information for interpreting secondary turnover. In our experiment, CUE showed a modest, but not statistically significant, decrease from ~0.70 at 6 h to ~0.60 at 168 h (Fig. S5). Similar apparent declines have been reported elsewhere (Geyer et al., 2019) and are generally interpreted not as true changes in microbial CUE, but as the consequence of turnover of substrate-derived biomass: respiration arising from the mineralisation of labelled biomass is still counted as "substrate-derived respiration" in the standard partitioning approach. As a result, tracer-based CUE estimates tend to decrease over time even when CUE itself remains constant (Hagerty et al., 2014; Geyer et al., 2019). The lack of a statistically significant decline observed here is therefore consistent with limited secondary turnover during the incubation.

Nevertheless, within conceptual frameworks that regard long-term SOC as being dominated by mineral-associated microbial residues rather than undecomposed plant litter (Schmidt et al., 2011; Lehmann and Kleber, 2015), $y0$ remains a potentially useful descriptor for tracking the fate of substrate-derived microbial residues across different soil types, or environmental conditions (Geyer et al., 2016). While the model represents this secondary turnover as a linear process for simplicity, a second exponential rise to an asymptote would more realistically reflect the finite size of the residue pool.

### 4.2. Comparison between the two-component model method and the partitioning method

The difference (0.10) between CUE values derived from the two-component model (0.80) and the $^{13}C$-biomass/$CO_2$ partitioning method (0.70) was statistically significant (Welch's *t*-test) at the 95 % level ($p = 0.0495$), indicating that the two methods are not functionally equivalent or directly comparable, as they capture different aspects of microbial carbon allocation. The two-component model CUE is above the interquartile range (0.44–0.76) reported by Qiao et al. (2019) in a meta-analysis of 289 glucose-based CUE measurements. The higher CUE value derived from the two-component model approach, based only on $^{13}C$-$CO_2$ flux data, may reflect its more comprehensive accounting, by mass balance, of C allocated to biosynthesis.

When carbon partitioning was examined at 6 h, the time point used to calculate CUE in the $^{13}C$-biomass/$CO_2$ partitioning method, 14 % of the added glucose-derived carbon had been mineralised, while 72 % was quantified in the soil organic carbon (SOC) pool. Of this SOC pool, 46 % could be accounted for as microbial biomass carbon (after using $k_{EC}$ to correct for extractable microbial biomass C) and ~1 % as unfumigated $K_2SO_4$-extractable organic carbon. This leaves ~53 % of the glucose-derived C in the SOC unaccounted for in biomass or extractable fractions. When extending to the full incubation period (1–168 h), the glucose-derived carbon content of SOC was approximately twice that of glucose-derived microbial biomass carbon (Fig. 4). This discrepancy resulted in a mass balance of approximately 87 % when $^{13}C$-glucose-C allocated to $CO_2$-C and SOC were summed, which is within the typical range for soil C tracing methods (Gougoulias et al., 2018; Geyer et al., 2019). When glucose-C allocated to $CO_2$-C, microbial biomass carbon, and non-fumigated $K_2SO_4$ extractable organic carbon were summed, the mass balance was only approximately 54 %. These mass-balance calculations suggest that a substantial fraction of substrate-derived biosynthetic carbon is retained in SOC pools that are not captured by the combination of microbial biomass carbon and non-fumigated $K_2SO_4$-extractable organic carbon used in the $^{13}C$-biomass/$CO_2$ partitioning approach.

As alluded to earlier, soil microorganisms allocate carbon not only to intracellular biomass but also extracellular biosynthetic products, such as extracellular polymeric substances (EPS), including exoenzymes, and also other secreted products (van Bodegom, 2007; Flemming and Wingender, 2010). Geyer et al. (2020) reported that soil microorganisms can generate extracellular products (residues) as rapidly as intracellular biomass, particularly in response to nutrient acquisition demands or community competition (Maynard et al., 2017; Joergensen and Wichern, 2018). Extracellular products can constitute up to 20 % of the total microbial carbon allocation, depending on microbial strategy and environmental conditions (Warren, 2020; Olagoke et al., 2022; Domeignoz-Horta et al., 2023). Bölscher et al. (2024) highlights that failing to account for extracellular enzymes (Domeignoz-Horta et al., 2023) and extracellular polymeric substances (Olagoke et al., 2022) can lead to the underestimation of CUE by up to 0.19 and 0.12, respectively. EPS are likely not quantified as biomass in MBC measurements because, in theory, as extracellular compounds, they are not released by chloroform lysis during the biomass fumigation–extraction method. They may also be largely absent from non-fumigated $K_2SO_4$ extracts, as EPS are often tightly bound to soil particles or microbial surfaces and require extraction protocols harsher than neutral salt washes (Redmile-Gordon et al., 2014; Wang et al., 2019). Thus, the widely used $^{13}C$-biomass/$CO_2$

partitioning method captures only the intracellular component of microbial biosynthesis and systematically underestimates CUE when CUE is defined, as in this study, to include both intra- and extracellular biomass-derived product (Dijkstra et al., 2022; Bölscher et al., 2024). The ~0.10 higher CUE we obtained relative to the $^{13}$C-biomass/$CO_2$ partitioning method is therefore consistent with the methodological omission of extracellular products in the latter and helps explain why our estimate lies at the upper end of glucose-based CUE values reported in the literature (Hagerty et al., 2014; Geyer et al., 2019; Qiao et al., 2019), although comparable estimates have been reported elsewhere (0.79~0.99) (Roberts and Jones, 2012; Dijkstra et al., 2015; Farrell et al., 2015).

Another possible explanation for the difference in extract-based mass balance is the use of a fixed $k_{EC}$ factor to convert carbon rendered $K_2SO_4$ extractable by fumigation into soil microbial biomass. A $k_{EC}$ value of 0.45, originally obtained by empirically calibrating $K_2SO_4$ extractable C against independent estimates of microbial biomass carbon from chloroform fumigation–incubation or tracer-recovery experiments (Joergensen, 1996), is commonly applied. However, $k_{EC}$ values may vary considerably (between 0.23 and 0.84) depending on land use, soil type, microbial community structure, and the analytical methods used (Joergensen, 1996). Under the specific conditions of our study (sandy loam from permanent grassland field in southeast England) and substrate (glucose) a $k_{EC}$ factor of 0.24 would have resulted in a mass balance similar to the ~85 % achieved by summing SOC and mineralisation. Applying a single, fixed value across diverse soils is therefore unlikely to reflect true extraction efficiency and can bias $^{13}$C-based biomass measurements (Sparling and West, 1988; Joergensen, 1996), propagating uncertainty into CUE estimates.

Physiological dynamics during substrate pulses further complicate the use of a fixed $k_{EC}$. The standard $k_{EC}$ coefficient assumes steady-state biomass with stable extractability after fumigation (Joergensen, 1996). Glucose addition can trigger rapid growth and shifts in cell physiology (e.g., changes in cell size; Cesar and Huang, 2017), which may alter the efficiency of chloroform lysis and thus the fraction of labelled biomass extracted.

Our two-component model, by relying solely on $^{13}$C-$CO_2$ dynamics and not on a fixed $k_{EC}$, avoids this source of uncertainty in MBC estimation and thus provides a CUE estimate that is less sensitive to assumptions about extraction efficiency and the partitioning of biosynthetic carbon in different microbial products.

### 4.3. Applicability and practical advantages of the two-component model method

From a practical standpoint, the mineralisation-based two-component model approach presents several operational advantages over the $^{13}$C-biomass/$CO_2$ partitioning method. It eliminates the need to measure microbial biomass using the fumigation-extraction method. This method is labour-intensive because it requires multiple steps that are sensitive to timing. Fumigation-extraction must be conducted on fresh, moist soil samples after the substrate addition and incubation, because drying or freezing may cause cell lysis, leading to an overestimation of extractable carbon in non-fumigated samples due to the release of intracellular carbon. Fresh extracts then require immediate analysis to avoid potential inaccuracies (Rhymes et al., 2021). Headspace gas samples can be stored and analysed later by GC and IRMS, since concentrations are stable over 28 days (Faust and Liebig, 2018). Fumigation–extraction also uses hazardous chloroform and must be carried out under a fume hood, limiting throughput and posing safety risks associated with desiccator evacuation (Vance et al., 1987). When $^{13}$C-labelled substrate tracing for CUE determination is used, additional technically demanding steps are needed to quantify $\delta^{13}$C in biomass extracts via isotope ratio mass spectrometry (IRMS). These include the removal of inorganic carbon, flushing the headspace with $CO_2$-free gas, and oxidizing the organic carbon in the extract to liberate it as $CO_2$ (Garcia-Pausas and Paterson, 2011). Overall, these factors make microbial biomass carbon determination operationally demanding and reduce its suitability for acquiring large datasets or its application to multi-location studies.

The two-component model method allows a complete CUE estimation to be conducted on samples within approximately two weeks by a single operator (including preparation, sampling, measurement), significantly enhancing sample throughput. The incubation setup and headspace gas sampling procedures are straightforward and do not require a high level of technical skill, facilitating easy adoption and scaling up of laboratory operations. Furthermore, an isotope-free estimate of parameter $a$ of 0.25 (Table S2) can be approximated from cumulative $CO_2$ differences between glucose-amended and control soils, eliminating isotope purchase and measurement costs (Fig. S4).

Statistically, the model has three degrees of freedom and can be fitted with as few as four time points if this still yields a reliable estimate of mineralisation for the asymptotic maximum (parameter $a$) of the first component. By reducing sampling times from 16 to around 8 time points (e.g. 1, 4, 6, 8, 24, 48, 96, 168 h) with three replicates each, the analytical workload can be halved compared with the data presented here without compromising accuracy. Although reducing sampling points improves experimental efficiency, it decreases the stability of parameters $a$, $b$ and $y0$ (Tables S3 and S4), and short-term (<1 week) incubations do not provide sufficient stability for reliable estimates of parameter $y0$. Studies employing the parameter $y0$ to trace the fate of microbial residues derived from specific substrates require longer-term measurements.

## 5. Conclusion

We applied a mineralisation-based two-component model to estimate substrate-specific microbial CUE using $^{13}$C-glucose. This approach avoids the need for $^{13}$C-biomass estimation via fumigation-extraction and a fixed conversion factor ($k_{EC}$) and additionally accounts for both intracellular and extracellular biosynthetic carbon. Compared to the commonly-used $^{13}$C-biomass/$CO_2$ partitioning method, it produced a higher CUE estimate (0.8 vs. 0.7) and mass balance (~87 % vs. ~54 %). The method eases post-incubation constraints and is suitable for comparative, higher-throughput screening under standardised incubations. The secondary turnover parameter $y0$ may also offer insights into the fate of substrate-derived microbial residues. This study represents a proof of concept demonstrating the feasibility of the approach using glucose in a temperate grassland soil. The CUE of 0.8 should be considered an upper-bound estimate specific to these incubation conditions, and its extension to other substrates or soil types requires validation.

## Declaration of generative AI and AI-assisted technologies in the manuscript preparation process

During the preparation of this work the authors used ChatGPT (GPT-5.3, OpenAI) in order to draft Python code for (i) generating schematic Fig. 1 and (ii) to conduct the sensitivity analysis reported in Supplementary Tables S3 and S4. They also used ChatGPT to generate ideas for improving clarity of writing. After using this tool, the authors reviewed and edited the content as needed and take full responsibility for the content of the published article.

## CRediT authorship contribution statement

**Hanqing Lin:** Conceptualization, Data curation, Formal analysis, Investigation, Methodology, Visualization, Writing – original draft. **Tom Sizmur:** Conceptualization, Project administration, Supervision, Writing – review & editing. **Liz J. Shaw:** Conceptualization, Supervision, Writing – review & editing.

## Declaration of competing interest

The authors declare the following financial interests/personal relationships which may be considered as potential competing interests: Editor of Soil Biology and Biochemistry (L.J. Shaw). The other authors declare that they have no known competing financial interests or personal relationships that could have appeared to influence the work reported in this paper.

## Appendix A. Supplementary data

Supplementary data to this article can be found online at https://doi.org/10.1016/j.soilbio.2026.110143.

## Data availability

Data for "A respiration-based method for estimating soil microbial carbon use efficiency" (Original data) (Mendeley Data)

## References


Balesdent, J., Mariotti, A., 1996. Measurement of soil organic matter turnover using $^{13}C$ natural abundance. Mass Spectrometry of Soils 41, 83–111.

Bardgett, R.D., Saggar, S., 1994. Effects of heavy metal contamination on the short-term decomposition of labelled [$^{14}C$]glucose in a pasture soil. Soil Biology and Biochemistry 26, 727–733.

Bölscher, T., Vogel, C., Olagoke, F.K., Meurer, K.H.E., Herrmann, A.M., Colombi, T., Brunn, M., Domeignoz-Horta, L.A., 2024. Beyond growth: the significance of non-growth anabolism for microbial carbon-use efficiency in the light of soil carbon stabilisation. Soil Biology and Biochemistry 193, 109400.

Brant, J.B., Sulzman, E.W., Myrold, D.D., 2006. Microbial community utilization of added carbon substrates in response to long-term carbon input manipulation. Soil Biology and Biochemistry 38, 2219–2232.

Cesar, S., Huang, K.C., 2017. Thinking big: the tunability of bacterial cell size. FEMS Microbiology Reviews 41, 672–678.

Coody, P.N., Sommers, L.E., Nelson, D.W., 1986. Kinetics of glucose uptake by soil microorganisms. Soil Biology and Biochemistry 18, 283–289.

Craig, M.E., Geyer, K.M., Beidler, K.V., Brzostek, E.R., Frey, S.D., Stuart Grandy, A., Liang, C., Phillips, R.P., 2022. Fast-decaying plant litter enhances soil carbon in temperate forests but not through microbial physiological traits. Nature Communications 13, 1229.

Del Giorgio, P.A., Cole, J.J., 1998. Bacterial growth efficiency in natural aquatic systems. Annual Review of Ecology and Systematics 29, 503–541.

Deutscher, J., Francke, C., Postma Pieter, W., 2006. How phosphotransferase system-related protein phosphorylation regulates carbohydrate metabolism in bacteria. Microbiology and Molecular Biology Reviews 70, 939–1031.

Dijkstra, P., Martinez, A., Thomas, S.C., Seymour, C.O., Wu, W., Dippold, M.A., Megonigal, J.P., Schwartz, E., Hungate, B.A., 2022. On maintenance and metabolisms in soil microbial communities. Plant and Soil 476, 385–396.

Dijkstra, P., Salpas, E., Fairbanks, D., Miller, E.B., Hagerty, S.B., van Groenigen, K.J., Hungate, B.A., Marks, J.C., Koch, G.W., Schwartz, E., 2015. High carbon use efficiency in soil microbial communities is related to balanced growth, not storage compound synthesis. Soil Biology and Biochemistry 89, 35–43.

Domeignoz-Horta, L.A., Pold, G., Erb, H., Sebag, D., Verrecchia, E., Northen, T., Louie, K., Eloe-Fadrosh, E., Pennacchio, C., Knorr, M.A., 2023. Substrate availability and not thermal acclimation controls microbial temperature sensitivity response to long-term warming. Global Change Biology 29, 1574–1590.

Farrell, M., Macdonald, L.M., Baldock, J.A., 2015. Biochar differentially affects the cycling and partitioning of low molecular weight carbon in contrasting soils. Soil Biology and Biochemistry 80, 79–88.

Faust, D.R., Liebig, M.A., 2018. Effects of storage time and temperature on greenhouse gas samples in exetainer vials with chlorobutyl septa caps. MethodsX 5, 857–864.

Fischer, H., Ingwersen, J., Kuzyakov, Y., 2010. Microbial uptake of low-molecular-weight organic substances out-competes sorption in soil. European Journal of Soil Science 61, 504–513.

Flemming, H.-C., Wingender, J., 2010. The biofilm matrix. Nature Reviews Microbiology 8, 623–633.

Frey, S.D., Lee, J., Melillo, J.M., Six, J., 2013. The temperature response of soil microbial efficiency and its feedback to climate. Nature Climate Change 3, 395–398.

Garcia-Pausas, J., Paterson, E., 2011. Microbial community abundance and structure are determinants of soil organic matter mineralisation in the presence of labile carbon. Soil Biology and Biochemistry 43, 1705–1713.

Geyer, K., Schnecker, J., Grandy, A.S., Richter, A., Frey, S., 2020. Assessing microbial residues in soil as a potential carbon sink and moderator of carbon use efficiency. Biogeochemistry 151, 237–249.

Geyer, K.M., Dijkstra, P., Sinsabaugh, R., Frey, S.D., 2019. Clarifying the interpretation of carbon use efficiency in soil through methods comparison. Soil Biology and Biochemistry 128, 79–88.

Geyer, K.M., Kyker-Snowman, E., Grandy, A.S., Frey, S.D., 2016. Microbial carbon use efficiency: accounting for population, community, and ecosystem-scale controls over the fate of metabolized organic matter. Biogeochemistry 127, 173–188.

Gommers, P.J., van Schie, B.J., van Dijken, J.P., Kuenen, J.G., 1988. Biochemical limits to microbial growth yields: an analysis of mixed substrate utilization. Biotechnology and Bioengineering 32, 86–94.

Gougoulias, C., Meade, A., Shaw, L.J., 2018. Apportioning bacterial carbon source utilization in soil using $^{14}C$ isotope analysis of fish-targeted bacterial populations sorted by fluorescence activated cell sorting (FACS): $^{14}C$-FISH-FACS. Environmental Microbiology Reports 10, 245–254.

Hagerty, S.B., van Groenigen, K.J., Allison, S.D., Hungate, B.A., Schwartz, E., Koch, G.W., Kolka, R.K., Dijkstra, P., 2014. Accelerated microbial turnover but constant growth efficiency with warming in soil. Nature Climate Change 4, 903–906.

Hill, P.W., Farrar, J.F., Jones, D.L., 2008. Decoupling of microbial glucose uptake and mineralization in soil. Soil Biology and Biochemistry 40, 616–624.

Islam, M.R., Singh, B., Dijkstra, F.A., 2023. Microbial carbon use efficiency of glucose varies with soil clay content: a meta-analysis. Applied Soil Ecology 181, 104636.

Jagadamma, S., Mayes, M.A., Steinweg, J.M., Schaeffer, S.M., 2014. Substrate quality alters the microbial mineralization of added substrate and soil organic carbon. Biogeosciences 11, 4665–4678.

Joergensen, R.G., 1996. The fumigation-extraction method to estimate soil microbial biomass: calibration of the kec value. Soil Biology and Biochemistry 28, 25–31.

Joergensen, R.G., Wichern, F., 2018. Alive and kicking: why dormant soil microorganisms matter. Soil Biology and Biochemistry 116, 419–430.

Lane, S., Xu, H., Oh, E.J., Kim, H., Lesmana, A., Jeong, D., Zhang, G., Tsai, C.-S., Jin, Y.-S., Kim, S.R., 2018. Glucose repression can be alleviated by reducing glucose phosphorylation rate in saccharomyces cerevisiae. Scientific Reports 8, 2613.

Lehmann, J., Kleber, M., 2015. The contentious nature of soil organic matter. Nature 528, 60–68.

Liang, Y., Leifheit, E.F., Lehmann, A., Rillig, M.C., 2025. Soil organic carbon stabilization is influenced by microbial diversity and temperature. Scientific Reports 15, 13990.

Manzoni, S., Čapek, P., Porada, P., Thurner, M., Winterdahl, M., Beer, C., Brüchert, V., Frouz, J., Herrmann, A.M., Lindahl, B.D., 2018. Reviews and syntheses: carbon use efficiency from organisms to ecosystems–definitions, theories, and empirical evidence. Biogeosciences 15, 5929–5949.

Manzoni, S., Taylor, P., Richter, A., Porporato, A., Ågren, G.I., 2012. Environmental and stoichiometric controls on microbial carbon-use efficiency in soils. New Phytologist 196, 79–91.

Mariano, E., Jones, D.L., Hill, P.W., Trivelin, P.C.O., 2016. Mineral nitrogen forms alter $^{14}C$-glucose mineralisation and nitrogen transformations in litter and soil from two sugarcane fields. Applied Soil Ecology 107, 154–161.

Maynard, D.S., Crowther, T.W., Bradford, M.A., 2017. Fungal interactions reduce carbon use efficiency. Ecology Letters 20, 1034–1042.

Nguyen, C., Guckert, A., 2001. Short-term utilisation of $^{14}C$-[U]glucose by soil microorganisms in relation to carbon availability. Soil Biology and Biochemistry 33, 53–60.

Olagoke, F.K., Bettermann, A., Nguyen, P.T.B., Redmile-Gordon, M., Babin, D., Smalla, K., Nesme, J., Sørensen, S.J., Kalbitz, K., Vogel, C., 2022. Importance of substrate quality and clay content on microbial extracellular polymeric substances production and aggregate stability in soils. Biology and Fertility of Soils 58, 435–457.

Porras, R.C., Hicks Pries, C.E., Torn, M.S., Nico, P.S., 2018. Synthetic iron (Hydr)oxide-glucose associations in subsurface soil: effects on decomposability of mineral associated carbon. Science of The Total Environment 613–614, 342–351.

Qiao, Y., Wang, J., Liang, G., Du, Z., Zhou, J., Zhu, C., Huang, K., Zhou, X., Luo, Y., Yan, L., Xia, J., 2019. Global variation of soil microbial carbon-use efficiency in relation to growth temperature and substrate supply. Scientific Reports 9, 5621.

Redmile-Gordon, M.A., Brookes, P.C., Evershed, R.P., Goulding, K.W.T., Hirsch, P.R., 2014. Measuring the soil-microbial interface: extraction of extracellular polymeric substances (EPS) from soil biofilms. Soil Biology and Biochemistry 72, 163–171.

Rhymes, J.M., Cordero, I., Chomel, M., Lavallee, J.M., Straathof, A.L., Ashworth, D., Langridge, H., Semchenko, M., de Vries, F.T., Johnson, D., Bardgett, R.D., 2021. Are researchers following best storage practices for measuring soil biochemical properties? Soil 7, 95–106.

Roberts, P., Jones, D.L., 2012. Microbial and plant uptake of free amino sugars in grassland soils. Soil Biology and Biochemistry 49, 139–149.

Roth, P., Jeckelmann, J.-M., Fender, I., Ucurum, Z., Lemmin, T., Fotiadis, D., 2024. Structure and mechanism of a phosphotransferase system glucose transporter. Nature Communications 15, 7992.

Satterthwaite, F.E., 1946. An approximate distribution of estimates of variance components. Biometric Bulletin 2, 110–114.

Schmidt, M.W.I., Torn, M.S., Abiven, S., Dittmar, T., Guggenberger, G., Janssens, I.A., Kleber, M., Kögel-Knabner, I., Lehmann, J., Manning, D.A.C., Nannipieri, P., Rasse, D.P., Weiner, S., Trumbore, S.E., 2011. Persistence of soil organic matter as an ecosystem property. Nature 478, 49–56.

Scow, K.M., Simkins, S., Alexander, M., 1986. Kinetics of mineralization of organic compounds at low concentrations in soil. Applied and Environmental Microbiology 51, 1028–1035.

Sinsabaugh, R.L., Manzoni, S., Moorhead, D.L., Richter, A., 2013. Carbon use efficiency of microbial communities: stoichiometry, methodology and modelling. Ecology Letters 16, 930–939.

Sparling, G.P., West, A.W., 1988. A direct extraction method to estimate soil microbial C: calibration in situ using microbial respiration and $^{14}C$ labelled cells. Soil Biology and Biochemistry 20, 337–343.

Tao, F., Huang, Y., Hungate, B.A., Manzoni, S., Frey, S.D., Schmidt, M.W.I., Reichstein, M., Carvalhais, N., Ciais, P., Jiang, L., Lehmann, J., Wang, Y.-P.,

Houlton, B.Z., Ahrens, B., Mishra, U., Hugelius, G., Hocking, T.D., Lu, X., Shi, Z., Viatkin, K., Vargas, R., Yigini, Y., Omuto, C., Malik, A.A., Peralta, G., Cuevas-Corona, R., Di Paolo, L.E., Luotto, I., Liao, C., Liang, Y.-S., Saynes, V.S., Huang, X., Luo, Y., 2023. Microbial carbon use efficiency promotes global soil carbon storage. Nature 618, 981–985.

van Bodegom, P., 2007. Microbial maintenance: a critical review on its quantification. Microbial Ecology 53, 513–523.

Vance, E.D., Brookes, P.C., Jenkinson, D.S., 1987. An extraction method for measuring soil microbial biomass C. Soil Biology and Biochemistry 19, 703–707.

Waldrop, M.P., Firestone, M.K., 2004. Microbial community utilization of recalcitrant and simple carbon compounds: impact of oak-woodland plant communities. Oecologia 138, 275–284.

Wang, C., Qu, L., Yang, L., Liu, D., Morrissey, E., Miao, R., Liu, Z., Wang, Q., Fang, Y., Bai, E., 2021. Large-scale importance of microbial carbon use efficiency and necromass to soil organic carbon. Global Change Biology 27, 2039–2048.

Wang, S., Redmile-Gordon, M., Mortimer, M., Cai, P., Wu, Y., Peacock, C.L., Gao, C., Huang, Q., 2019. Extraction of extracellular polymeric substances (EPS) from red soils (ultisols). Soil Biology and Biochemistry 135, 283–285.

Warren, C.R., 2020. Pools and fluxes of osmolytes in moist soil and dry soil that has been re-wet. Soil Biology and Biochemistry 150, 108012.

Welch, B.L., 1947. The generalization of 'student's' problem when several different population varlances are involved. Biometrika 34, 28–35.

Wijnants, S., Riedelberger, M., Penninger, P., Kuchler, K., Van Dijck, P., 2020. Sugar phosphorylation controls carbon source utilization and virulence of candida albicans. Frontiers in Microbiology 11, 2020.

Zhang, F., Wang, Q., Zhang, Y., Yao, S., Wang, Q., Ndzana, G., Hamer, U., Kuzyakov, Y., Zhang, B., 2024. Soil organic carbon increase via microbial assimilation or soil protection against the priming effect is mediated by the availability of soil N relative to input C. Geoderma 444, 116861.